# RESEARCH PAPER

# Phase I and II metabolism and MRP2-mediated export of bosentan in a MDCKII-OATP1B1-CYP3A4-UGT1A1-MRP2 quadruple-transfected cell line

C Fahrmayr[1], J König[1], D Auge[1], M Mieth[1], K Münch[1], J Segrestaa[2], T Pfeifer[2], A Treiber[2] and MF Fromm[1]

[1]*Institute of Experimental and Clinical Pharmacology and Toxicology, Friedrich-Alexander-Universität Erlangen-Nürnberg, Erlangen, Germany, and* [2]*Actelion Pharmaceuticals Ltd, Allschwil, Switzerland*

## BACKGROUND AND PURPOSE

Hepatic uptake (e.g. by OATP1B1), phase I and II metabolism (e.g. by CYP3A4, UGT1A1) and subsequent biliary excretion (e.g. by MRP2) are key determinants for the pharmacokinetics of numerous drugs. However, stably transfected cell models for the simultaneous investigation of transport and phase I and II metabolism of drugs are lacking.

## EXPERIMENTAL APPROACH

A newly established quadruple-transfected MDCKII-OATP1B1-CYP3A4-UGT1A1-MRP2 cell line was used to investigate metabolism and transcellular transport of the endothelin receptor antagonist bosentan.

## KEY RESULTS

Intracellular accumulation of bosentan equivalents (i.e. parent compound and metabolites) was significantly lower in all cell lines expressing MRP2 compared to cell lines lacking this transporter ($P < 0.001$). Accordingly, considerably higher amounts of bosentan equivalents were detectable in the apical compartments of cell lines with MRP2 expression ($P < 0.001$). HPLC and LC-MS measurements revealed that mainly unchanged bosentan accumulated in intracellular and apical compartments. Furthermore, the phase I metabolites Ro 48–5033 and Ro 47–8634 were detected intracellularly in cell lines expressing CYP3A4. Additionally, a direct glucuronide of bosentan could be identified intracellularly in cell lines expressing UGT1A1 and in the apical compartments of cell lines expressing UGT1A1 and MRP2.

## CONCLUSIONS AND IMPLICATIONS

These *in vitro* data indicate that bosentan is a substrate of UGT1A1. Moreover, the efflux transporter MRP2 mediates export of bosentan and most likely also of bosentan glucuronide in the cell system. Taken together, cell lines simultaneously expressing transport proteins and metabolizing enzymes represent additional useful tools for the investigation of the interplay of transport and metabolism of drugs.

## Abbreviations

CYP3A4, cytochrome P450 enzyme 3A4; Mrp2/MRP2, rodent/human multidrug resistance protein 2; OATP1B1, organic anion transporting polypeptide 1B1; Ro 47–8634, 4-*tert*-butyl-*N*-[6-(2-hydroxy-ethoxy)-5-(2-hydroxy-phenoxy)-[2,2']bipyrimidinyl-4-yl]-benzenesulfonamide; Ro 48–5033, 4-(2-hydroxy-1,1-dimethyl-ethyl)-*N*-[6-(2-hydroxy-ethoxy)-5-(2-methoxy-phenoxy)-[2,2']bipyrimidinyl-4-yl]-benzenesulfonamide; Ro 64–1056, 4-(2-hydroxy-1,1-dimethyl-ethyl)-*N*-[6-(2-hydroxy-ethoxy)-5-(2-hydroxy-phenoxy)-[2,2']bipyrimidinyl-4-yl]-benzenesulfonamide; RT-PCR, reverse transcriptase polymerase chain reaction; *SLCO,* solute carrier family of the OATPs; UGT1A1, uridine diphosphate-glucuronosyltransferase 1A1

## Introduction

The coordinate process of drug uptake into hepatocytes, intracellular drug metabolism and the subsequent excretion of drug metabolites into bile is an important determinant for the pharmacokinetics and pharmacodynamics of orally administered drugs. Organic anion transporting polypeptides (OATPs) such as OATP1B1 (gene symbol: *SLCO1B1*) play an important role in the uptake process of drugs from portal venous blood into hepatocytes (König, 2011). Following hepatic uptake, drugs often undergo phase I and/or phase II metabolism reactions [e.g. by cytochrome P450 enzyme 3A4 (*CYP3A4*) and/or uridine diphosphate-glucuronosyl transferase 1A1 (*UGT1A1*)] and drugs or their metabolites are subsequently exported into bile by efflux transporters, for example by MRP2, a member of the ABCC transporter family [gene symbol: *ABCC2*; (Ho and Kim, 2005; Funk, 2008; Zolk and Fromm, 2011)].

Bosentan, a dual endothelin receptor antagonist with high affinity for both endothelin A and B receptors, was approved as first oral treatment for pulmonary arterial hypertension (Clozel *et al.*, 1994; Weber *et al.*, 1996; van Giersbergen *et al.*, 2002; Treiber *et al.*, 2007; Thorin and Clozel, 2010). It is metabolized *in vitro* to a similar extent by CYP3A4 and by CYP2C9 and the known resulting metabolites are a phenol metabolite (4-*tert*-butyl-*N*-[6-(2-hydroxy-ethoxy)-5-(2-hydroxy-phenoxy)-[2,2′]bipyrimidinyl-4-yl]-benzenesulfonamide; Ro 47–8634), a hydroxy metabolite (4-(2-hydroxy-1,1-dimethyl-ethyl)-*N*-[6-(2-hydroxy-ethoxy)-5-(2-methoxy-phenoxy)-[2,2′]bipyrimidinyl-4-yl]-benzenesulfonamide; Ro 48–5033) and a secondary metabolite containing both biochemical modifications [4-(2-hydroxy-1,1-dimethyl-ethyl)-*N*-[6-(2-hydroxy-ethoxy)-5-(2-hydroxy-phenoxy)-[2,2′]bipyrimidinyl-4-yl]-benzenesulfonamide; Ro 64–1056, (Weber *et al.*, 1999c; van Giersbergen *et al.*, 2002; Treiber *et al.*, 2007)]. Among these metabolites, only the hydroxy metabolite is pharmacologically active. The parent compound and the hydroxy metabolite are substrates of OATP1B1 [with a $K_m$ value of 44 μM for bosentan and a $K_m$ value of 60 μM for the hydroxy metabolite; (Treiber *et al.*, 2007)]. The formation of glucuronide conjugates of the parent compound and its phase I metabolites in primary human hepatocytes has been discussed in an abstract (Shen *et al.*, 2009), but to the best of our knowledge, it is not known which UGT isoform(s) mediate(s) these reactions. Biliary excretion of bosentan metabolites and possibly of the parent compound accounts for more than 90% of total drug elimination (Weber *et al.*, 1999b; Treiber *et al.*, 2004). Fouassier *et al.* (2002) showed that bosentan alters canalicular bile formation predominantly via multidrug resistance protein 2 (Mrp2)-mediated mechanisms. However, the efflux transporter(s) mediating biliary secretion of bosentan and bosentan metabolites has/have not been identified.

To test the hypothesis whether bosentan and/or its phase I metabolites are substrates of the phase II enzyme UGT1A1 and that the excretion of the parent compound and/or possibly formed conjugates is mediated by MRP2, we generated and characterized a quadruple-transfected cell line with the simultaneous expression of the uptake transporter OATP1B1, the metabolizing enzymes CYP3A4 and UGT1A1 and the hepatic efflux transporter MRP2.

## Methods

### *Cloning of the human CYP3A4 cDNA*

Cloning of the CYP3A4 coding sequence (NM_017460.3) by reverse transcription PCR using human liver cDNA synthesized from a Multiple RNA panel (Clontech, Heidelberg, Germany) was performed as described earlier (Fahrmayr *et al.*, 2012). Amplification of the full length *CYP3A4* cDNA was conducted using the primer pair oCYP3A4-5′.for (5′-AGA TCT GTA AGG AAA GTA GTG ATG G-3′) and oCYP3A4-RT.rev (5′-AGC AGA TCT CCT TAG GAA AAT TCA G-3′), and the amplified fragment was cloned into the pCR2.1-TOPO vector (Invitrogen GmbH, Karlsruhe, Germany). After sequence verification (AGOWA, Berlin, Germany), the *CYP3A4* cDNA was cloned into the expression vector pVITRO1-blasti-mcs (InvivoGen, San Diego, CA, USA). Five base pair exchanges resulting in amino acid exchanges compared to the reference sequence were corrected using the QuikChange Lightning Multi Site-Directed Mutagenesis Kit (Stratagene, Amsterdam, The Netherlands). Finally, correctness and orientation of the cDNA were verified by sequencing (AGOWA).

### *Generation of stably transfected cells*

Generation and characterization of MDCKII-Co, MDCKII-OATP1B1, MDCKII-OATP1B1-UGT1A1, MDCKII-OATP1B1-MRP2 and MDCKII-OATP1B1-UGT1A1-MRP2 cell lines have been described before (Cui *et al.*, 1999; König *et al.*, 2000; Fehrenbach *et al.*, 2003; Fahrmayr *et al.*, 2012). For generation of the MDCKII-OATP1B1-CYP3A4-UGT1A1 and the MDCKII-OATP1B1-CYP3A4-MRP2 triple-transfected and the MDCKII-OATP1B1-CYP3A4-UGT1A1-MRP2 quadruple-transfected cell lines, MDCKII-OATP1B1-UGT1A1, MDCKII-OATP1B1-MRP2 and MDCKII-OATP1B1-UGT1A1-MRP2 cells were transfected with the plasmid pVITRO1-blasti-mcs-CYP3A4 using the Effectene transfection reagent kit according to the manufacturer's instructions (Qiagen GmbH, Hilden, Germany) respectively. To obtain single colonies of all three transfectants, cells were treated additionally with blasticidin S (7 μg ml$^{-1}$) for several weeks. Colonies grown under selection were tested for their *CYP3A4* mRNA expression using reverse transcriptase (RT)-PCR and LightCycler-based quantitative RT-PCR (Roche Diagnostics-Applied Science, Mannheim, Germany) as described before (Mandery *et al.*, 2010). Primer pairs used for quantification of *CYP3A4* mRNA expression were oCYP3A4-RT.for (5′-GCA AGA AGA ACA AGG ACA ACA TAG A-3′) and oCYP3A4-RT.rev (5′-AGC AGA TCT CCT TAG GAA AAT TCA G-3′) resulting in a 275 bp-fragment. Cell clones exhibiting the highest CYP3A4 expression of all three transfectants as well as the remaining cell lines used in this study (MDCKII-Co, MDCKII-OATP1B1, MDCKII-OATP1B1-MRP2, MDCKII-OATP1B1-UGT1A1-MRP2) were finally screened for their *SLCO1B1* mRNA (encoding OATP1B1), their *CYP3A4* mRNA (encoding CYP3A4), their *UGT1A1* mRNA (encoding UGT1A1) and their *ABCC2* mRNA (encoding MRP2) expression for comparative analysis. Primers used for quantitative real-time PCR have been described before (Fahrmayr *et al.*, 2012). All expression values were calculated in relation to the expression of the housekeeping gene *β-actin*. Cell clones showing the highest *CYP3A4* mRNA expression and a

*SLCO1B1*, *UGT1A1* and *ABCC2* mRNA expression comparable to the respective expression in the control cell lines (MDCKII-OATP1B1, MDCKII-OATP1B1-MRP2 and MDCKII-OATP1B1-UGT1A1-MRP2) were selected for further experiments. The expression of the respective mRNAs and proteins in the quadruple-transfected MDCKII-OATP1B1-CYP3A1-UGT1A1-MRP2 cell line and in all control cell lines has been analysed by quantitative RT-PCR and immunoblot analyses at different time points during these experiments demonstrating a stable expression over time for all transfected proteins.

## Immunoblot analysis

Generation of total protein homogenates and immunoblot analysis were performed as described previously (Seithel *et al.*, 2007; Mandery *et al.*, 2010). Five micrograms of cell homogenates used for detection of all four proteins (OATP1B1, CYP3A4, UGT1A1 and MRP2) were diluted with Laemmli buffer (62 mM Tris-HCl, 2% SDS, 10% glycerol, 0.01% bromphenol blue, and 0.4 mM dithiothreitol) and incubated for 5 min at 95°C, except for MRP2 samples (Cui *et al.*, 1999). Separation of total homogenates was conducted with 7.5 (for MRP2) and 10% (for OATP1B1, CYP3A4 and UGT1A1) SDS-polyacrylamide gels. An unstained protein ladder (Protein Ladder 10–250 kDa, New England BioLabs, Frankfurt am Main, Germany) was used to visualize the protein molecular weight ranges. After separation, proteins were transferred onto a nitrocellulose membrane (Protran, Whatman GmbH, Dassel, Germany) using a tank blotting system from Bio-Rad Laboratories (Munich, Germany). Membranes were then incubated with a purified rabbit polyclonal anti-human OATP1B1 antiserum [pESL; 1:500; (König *et al.*, 2000)], with a CYP3A4 purified MaxPab mouse polyclonal antibody (B01P; 1:1000; Abnova, Taipei, Taiwan), with a rabbit polyclonal anti-human UGT1A1 antibody (ab62600; 1:400; Abcam, Cambridge, UK) and with a rabbit polyclonal anti-human MRP2 antibody [EAG5; 1:5000; kindly provided by Professor Dr. Dietrich Keppler; DKFZ, Heidelberg, Germany; (Keppler and Kartenbeck, 1996; Jedlitschky *et al.*, 1997)]. Secondary antibodies were a horseradish peroxidase-conjugated goat anti-rabbit IgG (GE Healthcare UK Ltd, Little Chalfont, Buckinghamshire, UK) used at a 1:10 000 dilution (Seithel *et al.*, 2007) and horseradish peroxidase-conjugated goat anti-mouse Fab fragments (Dianova, Hamburg, Germany) at a 1:4000 dilution. Proteins were visualized using ECL Western blotting detection reagents (GE Healthcare UK Ltd) with the ChemiDoc XRS imaging system (Bio-Rad Laboratories). To detect β-actin, membranes were thereafter stripped and reincubated with a mouse monoclonal anti-human β-actin antibody (1:10 000; Sigma-Aldrich Chemie GmbH, Munich, Germany) and developed as described above. Different amounts of homogenate of the MDCKII-OATP1B1-CYP3A4-UGT1A1-MRP2 quadruple-transfected cell line further served as positive controls and for semiquatitative analysis of immunoblots. Blots were analysed using the Quantity One Software (Bio-Rad Laboratories).

## Determination of microsomal enzyme activities

Before transfection with the plasmid pVITRO1-blasti-mcs-CYP3A4, the cell lines MDCKII-OATP1B1, MDCKII-OATP1B1-MRP2 and MDCKII-OATP1B1-UGT1A1-MRP2 (Fahrmayr *et al.*, 2012) were tested for their NADPH-cytochrome P450 reductase activity. Measurement of the NADPH-cytochrome P450 reductase activity was performed as described (Gomes *et al.*, 2009). Instead of cytochrome P450, the NADPH-cytochrome P450 reductase can also reduce cytochrome c, which can be measured photometrically at 550 nm. In brief, 150 μg of total cell homogenates were equilibrated for 3 min at 25°C in 300 mM sodium phosphate buffer (pH 7.7), 1 mM KCN and 40 μM cytochrome c. Reduction of cytochrome c was started by addition of 100 μM NADPH and reduced cytochrome c was determined photometrically at 550 nM using a Bio-Rad SmartSpec™Plus spectrophotometer (Bio-Rad Laboratories) for 3 min as described previously (Vermilion and Coon, 1978; Tamura *et al.*, 1992; Dudka *et al.*, 2005). Enzyme activity was calculated using the extinction coefficient (ε) of 21 mM$^{-1}$ cm$^{-1}$ (Vermilion and Coon, 1978; Dudka *et al.*, 2005) and expressed as pmol of cytochrome c reduced per mg of total protein homogenates per min.

The activity of cytochrome P450 3A4 in the cell lines expressing this enzyme as well as in the control cell lines was assessed by measuring the amount of formed α-hydroxymidazolam after addition of the parent compound to the cell lines. Experiments were performed as described previously (Glaeser *et al.*, 2002) with some minor modifications. In brief, 100 μg of total protein homogenates were incubated either with 3 or 250 μM midazolam in 50 mM potassium hydrogen phosphate buffer (pH 7.4), 30 mM magnesium chloride and 4.8 mM NADPH in a total volume of 250 μL. Samples were equilibrated for 2 min at 37°C and the reaction was started by addition of NADPH. After 5 min, the reaction was stopped by addition of 500 μL of acetonitrile and samples were immediately stored at −80°C. The concentration of formed α-hydroxymidazolam was determined by LC-MS/MS.

## Quantification of α-hydroxymidazolam by LC-MS/MS

Concentrations of α-hydroxymidazolam from cell lysates were measured by means of HPLC-MS-MS [Agilent 1100 HPLC System (Agilent Technologies, Waldbronn, Germany); API 4000 (Applied Biosystems, Darmstadt, Germany)]. For sample preparation, 50 μL internal standard solution [d4-α-hydroxymidazolam (50 ng ml$^{-1}$ in acetonitrile)] was added to 50 μL sample. After mixing and centrifugation, 50 μL of the supernatant was diluted with 50 μL mobile phase [12 mM ammonium acetate with acetonitrile (1:1, v/v)]. Standards and quality controls in similar matrix were prepared identically to the samples. A ZORBAX Eclipse XDB C18 (150 mm × 4.6 mm, particle size 5 μm; Agilent Technologies) with a precolumn AQ C18 (4 mm × 3 mm; Phenomenex Ltd, Aschaffenburg, Germany) was installed as separation column. Chromatography was carried out isocratically at a flow rate of 0.6 mL min$^{-1}$. A valco valve behind the separation column was applied for cutting of salt (0.0–4.5 min waste; 4.5–6.5 min detection; 6.5–7.0 min waste). The mass transitions and collision energies were m/z 342.1 to 324.3 (31 eV) for α-hydroxymidazolam and m/z 346.0 to 328.1 (31 eV) for d4-α-hydroxymidazolam. The validated calibration range was between 0.1 and 100 ng mL$^{-1}$ and the lower limit of quantification was 0.1 ng mL$^{-1}$. The linear regression was weighted by 1/x. Correlation coefficients were at least 0.999. Intraday

coefficients of variation in cell lysate ranged from 2.0 to 6.1% and the intraday accuracies ranged from 3.9 to 15.7 both at concentrations of 0.1, 0.25, 50 and 100 ng mL$^{-1}$.

## Vectorial transport assays

Vectorial transport assays were performed as described (Cui *et al.*, 2001; Fehrenbach *et al.*, 2003; Fahrmayr *et al.*, 2012) with minor modifications. Briefly, MDCKII cells were seeded at an initial density of $4 \times 10^5$ cells·well$^{-1}$ onto ThinCerts (diameter 14 mm; pore size 0.4 μm; Greiner Bio-One GmbH, Frickenhausen, Germany) and grown for 3 days. Twenty-four hours prior to the vectorial transport experiments, cells were treated with 10 mM sodium butyrate (Merck KGaA, Darmstadt, Germany) to increase protein expression (Cui *et al.*, 1999). Radiolabelled bosentan was dissolved in uptake buffer (142 mM NaCl, 5 mM KCl, 1 mM K$_2$HPO$_4$, 1.2 mM MgSO$_4$, 1.5 mM CaCl$_2$, 5 mM glucose and 12.5 mM HEPES, pH 7.3) to a final concentration of 20 μM (4.5 kBq ml$^{-1}$) without addition of unlabelled bosentan. After washing with prewarmed (37°C) uptake buffer, 800 μL of uptake buffer were added to the apical compartment and 800 μL of uptake buffer containing bosentan were added to the basolateral compartment and cells were incubated at 37°C for 180 min. After 60 and 120 min, aliquots (100 μL) were removed from the apical compartment and plates were placed back to the incubator. After 180 min, additional 100 μL were taken from the apical compartment and radioactivity was measured by liquid scintillation counting (TriCarb 2800; PerkinElmer Life Sciences GmbH, Rodgau-Jügesheim, Germany). Afterwards, the cells were washed three times with ice-cold uptake buffer, filters were detached from the chambers and cells were lysed with 0.2% SDS. Small aliquots of lysates were both used to determine the intracellular accumulation of radioactivity by liquid scintillation counting and the protein concentrations by bicinchoninic acid assay (Pierce BCA Protein Assay Kit, Thermo Fisher Scientific Inc., Rockford, IL, USA).

For determination of bosentan and formed metabolites and for identification of possibly new phase II metabolites in vectorial transport assays, one assay was conducted as described above, with the exception that cells were incubated for 180 min without taking aliquots after 60 and 120 min. Samples from the intracellular and the apical compartments were measured by means of HPLC and LC-MS at Actelion Pharmaceuticals Ltd (Allschwil, Switzerland).

To investigate the transcellular leakage, cells were routinely treated likewise with 50 μM [³H]inulin.

Furthermore, apparent permeability coefficients (P$_{app}$) were calculated using the equation:

$$P_{app} = dQ/dt * (A^{-1} * C_o^{-1}) \,[cm\ s^{-1}]$$

where dQ/dt (μmol s$^{-1}$) is the initial transport rate (at 60 min), C$_0$ (μmol/cm³) the initial concentration in the donor chamber and A (cm²) the surface area of the monolayer (Artursson and Karlsson, 1991).

## Identification of bosentan and metabolites by HPLC/LC-MS

*HPLC method.* The analytical system consisted of two HPLC pumps LC-10AD VP equipped with a membrane degasser, a SCL-10AD VP system controller, a UV detector SPD-10AV VP

and an autosampler model SIL-HTc (all from Shimadzu, Reinach, Switzerland). The chromatographic separation of bosentan and its metabolites was achieved using a Phenomenex Luna C18 column (250 × 4.6 mm; particle size 5 μm; Phenomenex Ltd, Aschaffenburg, Germany) at 45°C with a flow rate of 1 mL min$^{-1}$. Mobile phases consisted of 50 mM ammonium formate adjusted to pH 4.0 with formic acid (phase A) and acetonitrile (phase B). The gradient method for the separation of bosentan and its metabolites was as follows: 0–10 min: 10% of phase B; 10–55 min: 25% of phase B; 55–60 min: 73% of phase B; 60–63 min: 95% of phase B; 63–64 min: 95% of phase B and 64–70 min: 10% of phase B. The run was stopped after 70 min. Due to the low levels of total radioactivity, post-column fractions were collected using an Agilent Technologies 1200 fraction collector (Agilent Technologies) in Deepwell LumaPlates™-96 (PerkinElmer) in intervals of 0.28 min, evaporated to dryness using an EZ-2 Evaporator (GeneVac Ltd, Ispwich, UK) and analysed offline using a TopCount-NXT™ microplate luminescence counter (PerkinElmer). Data processing was performed using the RadioStar software package (version 4.6, Berthold AG, Regensdorf, Switzerland). Using these chromatographic conditions, bosentan had a retention time of 41.0 min. The variability in retention time in the different chromatograms did not exceed 1 min over a total run time of 70 min.

*Mass spectrometry.* Structure identification was performed using a LTQ Orbitrap Velo Pro mass spectrometer (ThermoFinnigan, San Jose, CA, USA) coupled to a LC-20ADXR HPLC pump (Shimadzu). The mass spectrometer was operated in positive ion mode with the following instrument settings: ESI voltage 3.0 kV, capillary temperature 300°C, source temperature 200°C, sheath gas 40 psi, auxiliary gas 5 psi, capillary voltage 13 V, S-lens RF level 45%, mass range 190–1000 and a mass resolution of 30 000. The chromatographic method was identical to that described for the HPLC method with a 1:5 flow rate split. Data processing was performed using the Xcalibur 2.0.7 software package (Thermo Electron, San Jose, CA, USA).

*Data and statistical analysis.* Real-time PCR and immunoblot analysis determining mRNA and protein expression were repeated three times. Experiments determining the CYP3A4 enzyme activity were repeated two times on separate days with a total of four samples per concentration and cell line, and experiments determining the NADPH-reductase activity were performed on two separate days with a total of four samples per cell line. Each time point in transcellular transport experiments was investigated on two separate days with three wells per day (i.e. *n* = 6). For measurement of bosentan and formed metabolites by means of HPLC and LC-MS one transcellular transport experiment was performed with three wells per cell line (i.e. *n* = 3). All data are presented as mean ± SD. Multiple comparisons were analysed by ANOVA with subsequent Tukey-Kramer multiple comparison test by using Prism 3.01 (GraphPad Software, San Diego, CA, USA). A value of *P* < 0.05 was considered as statistically significant.

*Materials.* [¹⁴C]Bosentan (37 MBq ml$^{-1}$), unlabelled bosentan and bosentan metabolites were from Actelion Pharmaceuticals Ltd internal sources and [³H]inulin (74 MBq ml$^{-1}$) was

obtained from PerkinElmer Life Sciences GmbH (Rodgau-Jügesheim, Germany). Unlabelled inulin, poly-D-lysine hydrobromide and ammonium acetate were purchased from Sigma-Aldrich (Taufkirchen, Germany). Water-Baker analysed LC/MS reagent was from Mallinckrodt Baker B.V. (Deventer, The Netherlands). Liquid scintillation cocktail for HPLC analysis, Optiflow Safe 2, was purchased from Berthold Technologies GmbH. Sodium butyrate, cytochrome c and acetonitrile hypergrade for LC/MS were from Merck KGaA. The antibiotics zeocin, G418 (geniticin) disulfate and hygromycin were from Invitrogen (Groningen, the Netherlands) and the antibiotic blasticidin S was from InvivoGen. NADPH was obtained from AppliChem (Darmstadt, Germany) and midazolam was from Lipomed (Weil am Rhein, Germany). α-Hydroxymidazolam and the internal standard d4-α-hydroxymidazolam were purchased from LGC Standards

(Wesel, Germany). All other chemicals and reagents, unless stated otherwise, were obtained from Carl Roth GmbH + Co.KG (Karlsruhe, Germany) and were of the highest grade available.

## Results

### Expression analysis of OATP1B1, CYP3A4, UGT1A1 and MRP2 in single-, double-, triple- and quadruple-transfected cell lines

Figures 1 and 2 show the mRNA and protein expression of OATP1B1, CYP3A4, UGT1A1 and MRP2 in MDCKII-control cells (Co), single- (OATP1B1), double- (OATP1B1-MRP2), triple- (OATP1B1-CYP3A4-UGT1A1, OATP1B1-CYP3A4-
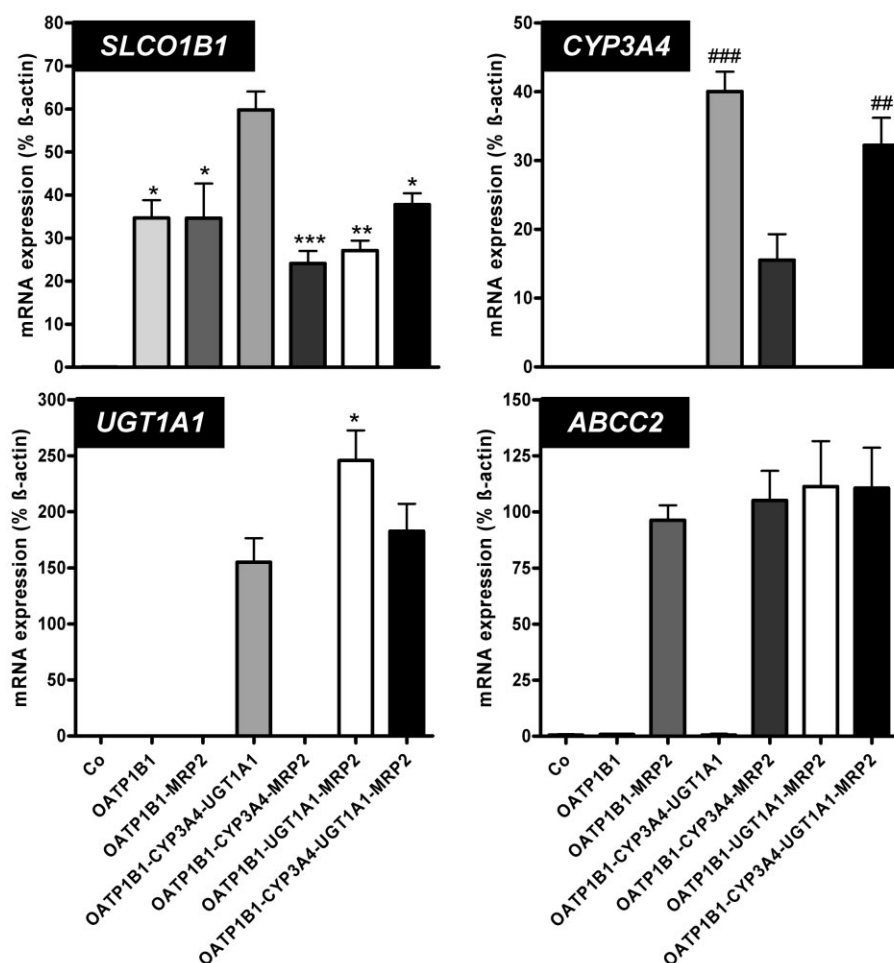


**Figure 1**

Quantitative real-time PCR (RT-PCR) analysis of *SLCO1B1* (encoding OATP1B1), *CYP3A4* (encoding CYP3A4), *UGT1A1* (encoding UGT1A1) and *ABCC2* (encoding MRP2) mRNA expression in MDCKII-control cells (Co), single- (OATP1B1), double- (OATP1B1-MRP2), triple- (OATP1B1-CYP3A4-UGT1A1, OATP1B1-CYP3A4-MRP2, OATP1B1-UGT1A1-MRP2) and quadruple-transfected (OATP1B1-CYP3A4-UGT1A1-MRP2) cell lines used in this study. The RT-PCR analysis was repeated three times and data are presented as mean ± SD in % *β-actin* mRNA expression. Statistical analyses were performed between the transfected cell lines among themselves. No expression of human *SLCO1B1*, *CYP3A4*, *UGT1A1* or *ABCC2* mRNA could be detected in MDCKII-control cells (Co). Multiple comparisons were analysed by ANOVA with subsequent Tukey–Kramer multiple comparison test. *$P < 0.05$, **$P < 0.01$, ***$P < 0.001$ versus MDCKII-OATP1B1-CYP3A4-UGT1A1 cells; ##$P < 0.01$, ###$P < 0.001$ versus MDCKII-OATP1B1-CYP3A4-MRP2 cells.
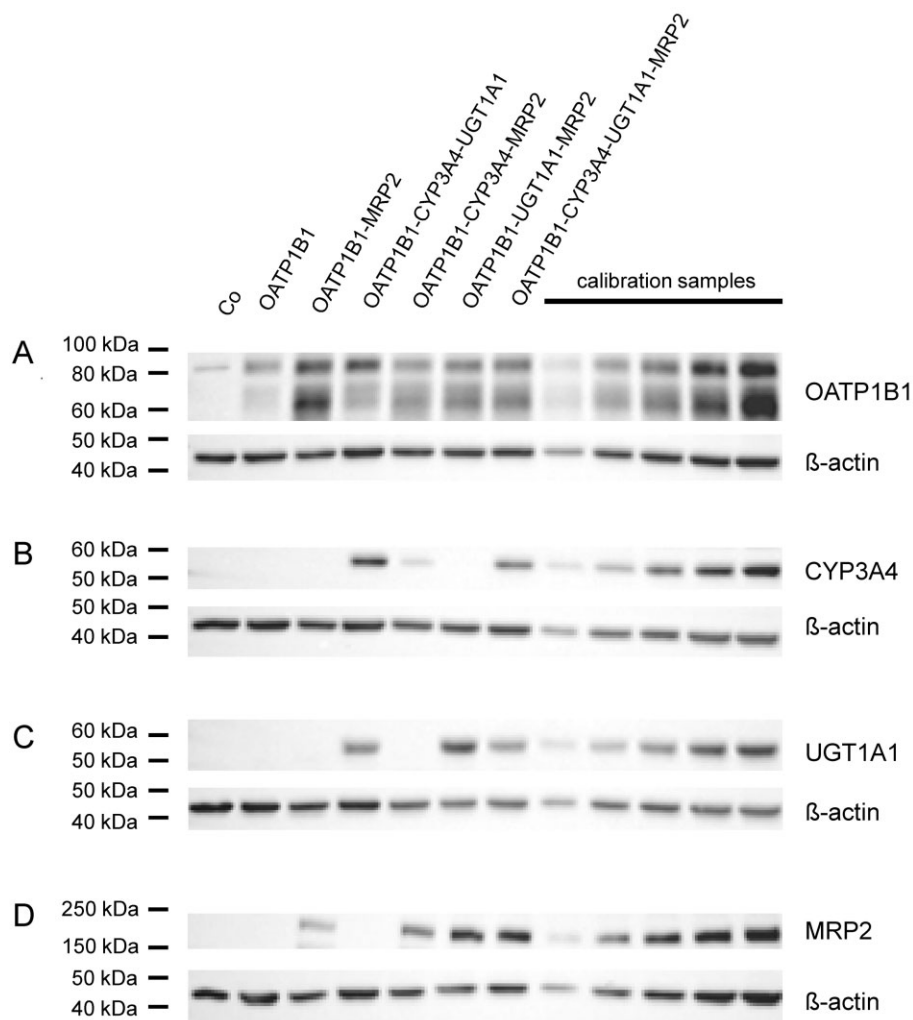
**Figure 2**
Immunoblot analyses of OATP1B1 (A), CYP3A4 (B), UGT1A1 (C) and MRP2 (D) expression in MDCKII-control cells (Co), single- (OATP1B1), double- (OATP1B1-MRP2), triple- (OATP1B1-CYP3A4-UGT1A1, OATP1B1-CYP3A4-MRP2, OATP1B1-UGT1A1-MRP2) and quadruple-transfected (OATP1B1-CYP3A4-UGT1A1-MRP2) cell lines used in this study. A 5-μg protein homogenate of each cell line was loaded. OATP1B1 shows one glycosylated form with an apparent molecular weight of 84 kDa and one unglycosylated form (58 kDa), CYP3A4 shows one band with approximately 55 kDa, UGT1A1 one with approximately 60 kDa and MRP2 one with 190 kDa. As positive controls and for semiquantitative analysis, calibration samples (1, 2.5, 5, 7.5 and 10 μg protein) of the quadruple-transfected cell line (OATP1B1-CYP3A4-UGT1A1-MRP2) were also loaded.

MRP2, OATP1B1-UGT1A1-MRP2) and quadruple-transfected cells (OATP1B1-CYP3A4-UGT1A1-MRP2). As expected, only transfected cell lines showed a respective mRNA and protein expression.

## Determination of microsomal enzyme activities

Prior to transfection with the plasmid pVITRO1-blasti-mcs-CYP3A4, cell lines were investigated for their NADPH-cytochrome P450 reductase activity, which is a prerequisite for CYP3A4 function. Net activity was between 11.1 and 14.5 nmol·mg protein$^{-1}$·min$^{-1}$ in the investigated cell lines with no significant differences.

Cytochrome P450 3A4 activity was determined via formation of the metabolite α-hydroxymidazolam (Figure 3) by LC-MS/MS after incubation of total homogenates of MDCKII-

control cells, single- (OATP1B1), double- (OATP1B1-MRP2), triple- (OATP1B1-CYP3A4-UGT1A1, OATP1B1-CYP3A4-MRP2, OATP1B1-UGT1A1-MRP2) and quadruple-transfected cells (OATP1B1-CYP3A4-UGT1A1-MRP2) with 3 μM (A) or 250 μM (B) midazolam (Figure 3). Only cell lines expressing the CYP3A4 enzyme showed formation of α-hydroxymidazolam, whereas no significant amounts were detectable in the other cell lines.

## Intracellular accumulation and vectorial transport of bosentan equivalents to the apical compartment of monolayers of MDCKII-control, single-, double-, triple- and quadruple-transfected cells

[14C]Bosentan was administered to the basal compartment of the cell monolayers of MDCKII-control (Co),
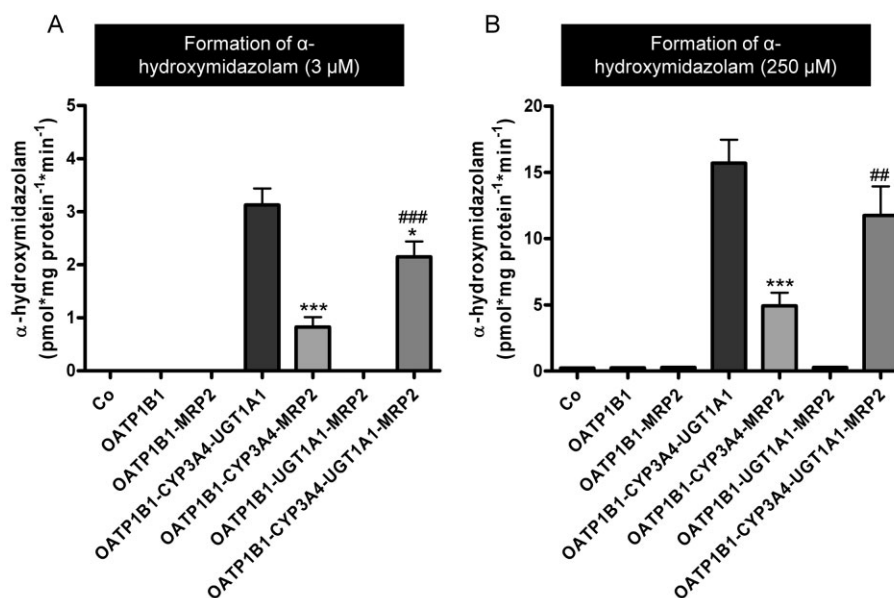
**Figure 3**

Determination of CYP3A4 enzyme activity in homogenates of MDCKII-control (Co), single- (OATP1B1), double- (OATP1B1-MRP2), triple-(OATP1B1-CYP3A4-UGT1A1, OATP1B1-CYP3A4-MRP2, OATP1B1-UGT1A1-MRP2) and quadruple-transfected (OATP1B1-CYP3A4-UGT1A1-MRP2) cell lines using midazolam assay. Total homogenates of cell lines were incubated with 3 μM midazolam (A) or 250 μM midazolam (B) at 37°C and the amount of the formed metabolite α-hydroxymidazolam was measured by LC-MS/MS. Statistical analyses were performed between the CYP3A4-transfected cell lines among themselves. Data are shown as mean value ± SD. *$P < 0.05$, ***$P < 0.001$ versus MDCKII-OATP1B1-CYP3A4-UGT1A1; ##$P < 0.01$, ###$P < 0.001$ versus MDCKII-OATP1B1-CYP3A4-MRP2 cells.

single- (OATP1B1), double- (OATP1B1-MRP2), triple-(OATP1B1-CYP3A4-UGT1A1, OATP1B1-CYP3A4-MRP2, OATP1B1-UGT1A1-MRP2) and quadruple-transfected cells (OATP1B1-CYP3A4-UGT1A1-MRP2). Figures 4 and 5 show the intracellular accumulation of bosentan equivalents (i.e. parent compound and metabolites) and the transcellular transport of bosentan equivalents into the apical compartment respectively. Intracellular accumulation of bosentan equivalents was significantly lower in cell lines expressing MRP2 (Figure 4; $P < 0.001$). Cell lines lacking MRP2 exhibited higher intracellular amounts of bosentan equivalents with the triple-transfected cell line MDCKII-OATP1B1-CYP3A4-UGT1A1 showing the highest amounts. In line with the lower intracellular values, higher amounts of bosentan equivalents were found in the apical compartment of monolayers of cell lines expressing MRP2 compared to cell lines without MRP2 expression at all investigated time points (Figure 5 A to C; $P < 0.001$). In MRP2-expressing cells apparent permeability ($P_{app}$) was more than 50% greater compared to $P_{app}$ in MDCKII-Co cells (4.3 [cm s$^{-1}$]*10$^{-6}$ in MDCKII-Co vs. 6.5, 7.5, 7.4 and 6.5 [cm s$^{-1}$]*10$^{-6}$ in MDCKII-OATP1B1-MRP2, MDCKII-OATP1B1-CYP3A4-MRP2, MDCKII-OATP1B1-UGT1A1-MRP2 and MDCKII-OATP1B1-CYP3A4-UGT1A1-MRP2 cells respectively; $P < 0.001$). Transcellular transport of bosentan equivalents to the apical compartment exhibited linear kinetics (Figure 6).

Qualitative measurements of samples from transcellular transport experiments by means of HPLC and LC-MS identified the phase I metabolites Ro 48–5033 and Ro 47–8634 in the intracellular compartments of cell lines expressing the phase I enzyme CYP3A4 (Table 1). The majority of radioac-tivity accumulating in the intracellular compartments consisted of bosentan itself. In addition to the phase I metabolites Ro 48–5033 and Ro 47–8634, bosentan glucuro-nide could be identified in the intracellular compartments of all cell lines expressing the phase II enzyme UGT1A1 (Table 1). Glucuronides of the phase I metabolites were not detected. Results of these measurements are summarized in Table 1. HPLC- and LC-MS-measurements revealed that mainly bosentan was translocated into the apical compart-ments of investigated cell lines confirming that bosentan itself is a substrate of MRP2. Furthermore, small amounts of bosentan glucuronide were detected in the apical compart-ments of cell lines expressing UGT1A1 and MRP2 indicating that also bosentan glucuronide is a substrate of MRP2.

## Discussion and conclusions

This study using a newly established quadruple-transfected MDCKII-OATP1B1-CYP3A4-UGT1A1-MRP2 cell line had the following major findings: (i) transporter-mediated uptake, phase I and II metabolism and efflux transport can be inves-tigated using this new cellular system. (ii) UGT1A1 is involved in formation of bosentan glucuronide. (iii) MRP2 mediates secretion of bosentan and most likely also of bosen-tan glucuronide.

In order to gain more insights into the hepatobiliary transport of drugs, their directed transport through mono-layers of cell lines stably expressing uptake as well as efflux transporters using *in vitro* cell models has intensively been
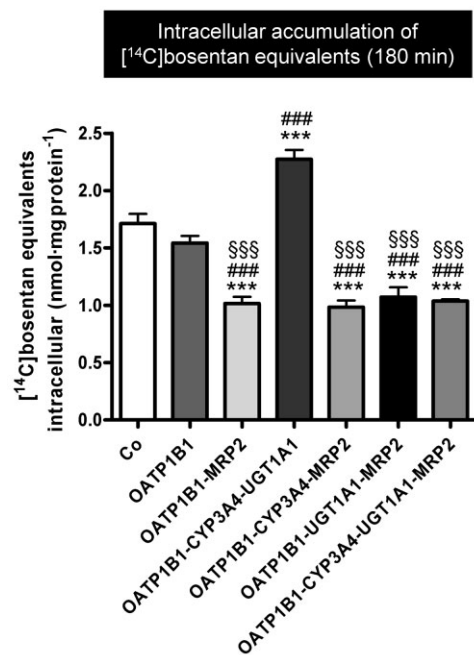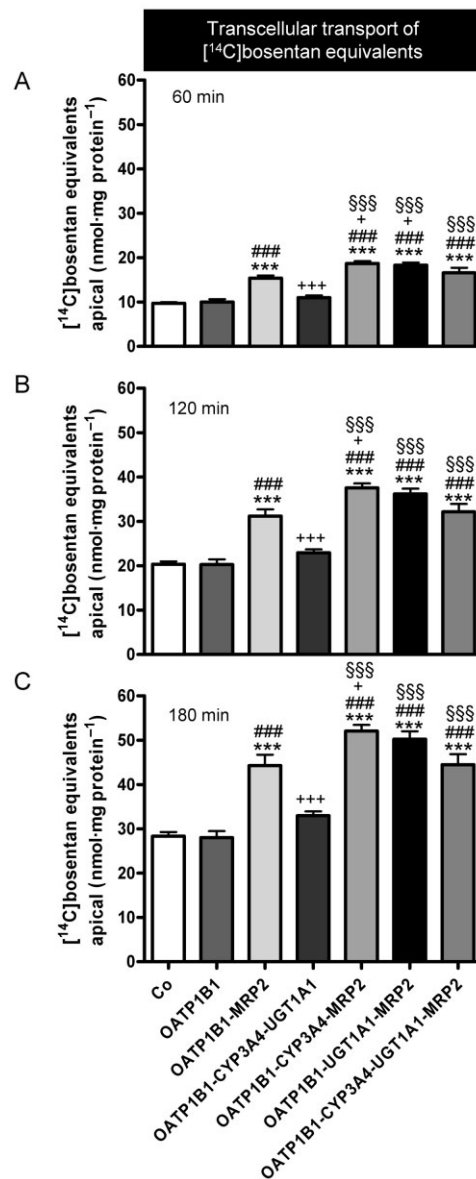
**Figure 4**

[$^{14}$C]Bosentan (20 μM) was administered to the basal compartment of monolayers of MDCKII-control (Co), single- (OATP1B1), double- (OATP1B1-MRP2), triple- (OATP1B1-CYP3A4-UGT1A1, OATP1B1-CYP3A4-MRP2, OATP1B1-UGT1A1-MRP2) and quadruple-transfected (OATP1B1-CYP3A4-UGT1A1-MRP2) cell lines. Intracellular accumulation of bosentan equivalents (i.e. parent compound and metabolites) in the cells after 180 min is shown. Data are shown as mean value ± SD. ***$P < 0.001$ versus MDCKII-Co; ###$P < 0.001$ versus MDCKII-OATP1B1; §§§$P < 0.001$ versus MDCKII-OATP1B1-CYP3A4-UGT1A1 cells.

studied (Cui *et al.*, 2001; Kopplow *et al.*, 2005; Ishiguro *et al.*, 2008; Nies *et al.*, 2008; Hirouchi *et al.*, 2009; König *et al.*, 2011). However, most drugs undergo phase I and/or phase II metabolism so that the coordinate process of drug transport and metabolism cannot be investigated using models expressing only transport proteins. Previously, experiments using an OATP1B1-UGT1A1-MRP2 triple-transfected cell line demonstrated that cell lines stably simultaneously expressing transport proteins and metabolizing enzymes provide useful tools to study the interplay of drug transport and drug metabolism (Fahrmayr *et al.*, 2012).

Based on the OATP1B1-UGT1A1-MRP2 triple-transfected cell line, we established and characterized a cell line with the additional expression of the phase I enzyme CYP3A4. For the characterization of this cell line, we used the dual endothelin receptor antagonist bosentan. *In vitro* and *in vivo* studies clearly revealed that the hepatic uptake transporters OATP1B1 and OATP1B3 as well as the cytochrome P450 enzymes CYP3A4 and CYP2C9 are important determinants of the disposition of bosentan (Treiber *et al.*, 2007; van Giersbergen *et al.*, 2007). In the present study, however, we could not detect a significant difference in the amount of radioactivity accumulating in the intracellular compartments of the OATP1B1 single-transfected cell line in comparison to the control cell line. This could be due to the much longer
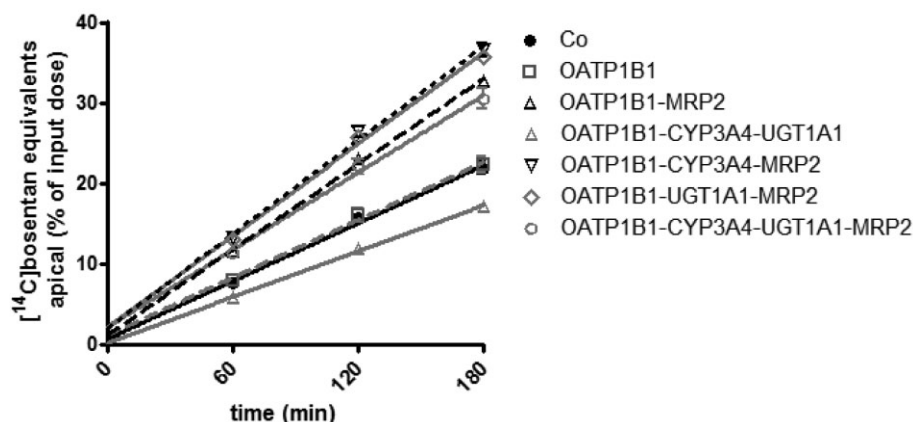


**Figure 5**

[$^{14}$C]Bosentan (20 μM) was administered to the basal compartment of monolayers of MDCKII-control (Co), single- (OATP1B1), double- (OATP1B1-MRP2), triple- (OATP1B1-CYP3A4-UGT1A1, OATP1B1-CYP3A4-MRP2, OATP1B1-UGT1A1-MRP2) and quadruple-transfected (OATP1B1-CYP3A4-UGT1A1-MRP2) cell lines. Translocation of bosentan equivalents into the apical compartment after 60 min (A), 120 min (B) and 180 min (C) is shown. Data are shown as mean value ± SD. ***$P < 0.001$ versus MDCKII-Co; ###$P < 0.001$ versus MDCKII-OATP1B1; +$P < 0.05$, +++$P < 0.001$ versus MDCKII-OATP1B1-MRP2; §§§$P < 0.001$ versus MDCKII-OATP1B1-CYP3A4-UGT1A1 cells.

incubation time in this study compared to uptake experiments leading to an increased contribution of additional transport processes (e.g. basolateral efflux).

Transcellular transport experiments using radiolabelled bosentan and subsequent liquid scintillation counting of intracellular samples revealed lower amounts of bosentan

**Figure 6**
[$^{14}$C]Bosentan (20 μM) was administered to the basal compartment of monolayers of MDCKII-control (Co), single- (OATP1B1), double- (OATP1B1-MRP2), triple- (OATP1B1-CYP3A4-UGT1A1, OATP1B1-CYP3A4-MRP2, OATP1B1-UGT1A1-MRP2) and quadruple-transfected (OATP1B1-CYP3A4-UGT1A1-MRP2) cell lines. Translocation of bosentan equivalents into the apical compartment after 60, 120 and 180 min is shown as percentage of administered radioactivity. All cell lines show linear transport kinetics.

equivalents (i.e. bosentan and possible metabolites) in cell lines expressing MRP2. Accordingly, significantly higher amounts of bosentan equivalents were detectable in the apical compartments of cell lines with an expression of MRP2 which demonstrated a contribution of MRP2 to the export of bosentan. To investigate this hypothesis, a further transcellular transport experiment was conducted with the subsequent measurement of samples by means of HPLC and LC-MS. In fact, these data revealed that mainly bosentan was transported into the apical compartments of the tested cell lines. Moreover, bosentan glucuronide was detected in the apical compartments of cell lines expressing UGT1A1 and MRP2 indicating a contribution of MRP2 to the translocation of the metabolite. It should be noted that significant amounts of bosentan equivalents were also detectable in MDCKII-control cells indicating that endogenous canine efflux transporters (e.g. canine Mrp2) also contribute to apical accumulation.
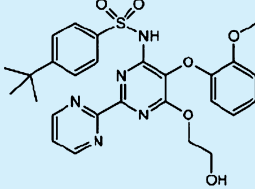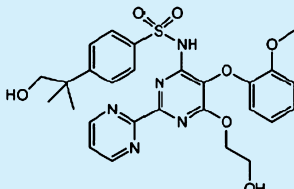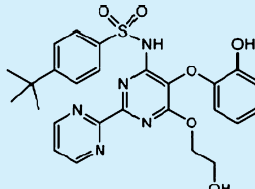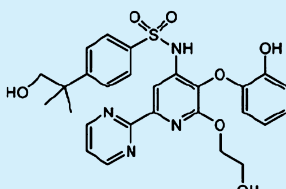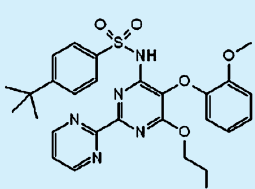
Several studies investigated the interaction of bosentan with transporters expressed in the canalicular membrane. However, none of them directly identified the transporter mediating biliary excretion of bosentan (Weber *et al.*, 1999a; Fattinger *et al.*, 2001; Fouassier *et al.*, 2002; Treiber *et al.*, 2004; Hartman *et al.*, 2010). *In vitro* studies conducted with primary human hepatocytes showed a decrease in the biliary elimination of the MRP2 substrate [2-D-Penicillamin, 5-D-penicillamine] enkephalin during simultaneous incubation with bosentan only in one of three donors (Hartman *et al.*, 2010). Furthermore, co-incubation experiments in primary human hepatocytes with bosentan and probenecid, a known inhibitor for MRP2, showed a reduced uptake and an increased elimination of bosentan (Hartman *et al.*, 2010). Moreover, Mano *et al.* (2007) reported that bosentan stimulated MRP2-mediated ATP-dependent vesicular transport of [$^{3}$H]estradiol. Thus, our study is the first one identifying unconjugated bosentan as substrate of MRP2. Although MRP2 is known as transporter of glutathione and glucuronide conjugates, MRP2-mediated, glutathione-dependent transport of the unconjugated anticancer agents etoposide,

vincristine and vinblastine has been shown (Cui *et al.*, 1999; van Aubel *et al.*, 1999; Evers *et al.*, 2000) suggesting a cotransport of these agents with glutathione (Jedlitschky *et al.*, 2006). Furthermore, a cotransport of drugs or endogenous substances with glutathione by other MRP transporters (MRP1 and MRP4) has also been shown (Rappa *et al.*, 1997; Cole and Deeley, 1998; Loe *et al.*, 1998; Rius *et al.*, 2006). Pilot experiments indicate that there is a trend towards higher total glutathione concentrations in the apical compartments of MDCKII-OATP1B1-MRP2 monolayers compared to the concentrations in the apical compartments of MDCKII-control cells after addition of bosentan (20 μM) to the respective basal compartments (data not shown).

The metabolism of bosentan by the cytochrome P450 enzymes CYP3A4 and CYP2C9 to three phase I metabolites (Ro 48–5033, Ro 47–8634 and Ro 64–1056) has been elucidated (van Giersbergen *et al.*, 2002; Treiber *et al.*, 2007). However, the glucuronidation of bosentan and its phase I metabolites by uridine diphosphate-glucuronosyltransferases has not been clarified in detail yet (Shen *et al.*, 2009). Transcellular transport experiments with labelled bosentan and measurement of samples by HPLC and LC-MS revealed the phase I metabolites Ro 48–5033 and Ro 47–8634 in the intracellular compartments of cell lines expressing the enzyme CYP3A4. However, the majority of radioactivity accumulating in the intracellular compartment of all cell lines consisted of bosentan itself. This could be due to the fact that bosentan is a rather poor substrate of CYP3A4 than the model substrate midazolam used to test the functionality of the enzyme in the cell lines. Shen *et al.* (2009) characterized the metabolism of bosentan to the phase I metabolites Ro 48–5033 and Ro 47–8634 in human liver microsomes and determined respective $K_m$ values of 65 μM (Ro 48–5033) and 73 μM (Ro 47–8634). In contrast, $K_m$ values for the metabolism of midazolam to α-hydroxymidazolam are 3.9 μM in human liver microsomes and 0.8 μM for recombinant CYP3A4 (Patki *et al.*, 2003).

## Table 1

Qualitative determination of bosentan and metabolites in the intracellular compartments of the investigated cell lines after transcellular transport experiments using [$^{14}$C]bosentan

| Identified compounds | | Co | OATP1B1 | OATP1B1-MRP2 | OATP1B1-CYP3A4-UGT1A1 | OATP1B1-CYP3A4-MRP2 | OATP1B1-UGT1A1-MRP2 | OATP1B1-CYP3A4-UGT1A1-MRP2 |
|---|---|---|---|---|---|---|---|---|
| Cell lines | | | | | | | | |
|  Bosentan | | + | + | + | + | + | + | + |
|  Ro 48–5033 | | – | – | – | + | + | – | + |
|  Ro 47–8634 | | – | – | – | + | + | – | + |
|  Ro 64–1056 | | n.d. | n.d. | n.d. | n.d. | n.d. | n.d. | n.d. |
|  Bosentan glucuronide | | – | – | – | + | – | + | + |

n.d., not detectable.

In addition to the phase I metabolites, bosentan glucuronide could be detected in cells with an expression of UGT1A1. Thus, a further metabolic reaction in the metabolic pathways of bosentan (i.e. direct glucuronidation of bosentan by UGT1A1) could be identified. A schematic representation of the extended metabolic pathway of bosentan is shown in

Figure 7. Glucuronides of the phase I metabolites, although possible on the basis of their chemical structure, could not be detected in the current study. This could be due to the fact that intracellular amounts of phase I metabolites were quite low, thus rendering the quantification of glucuronides of these metabolites was difficult. In accordance with our find-
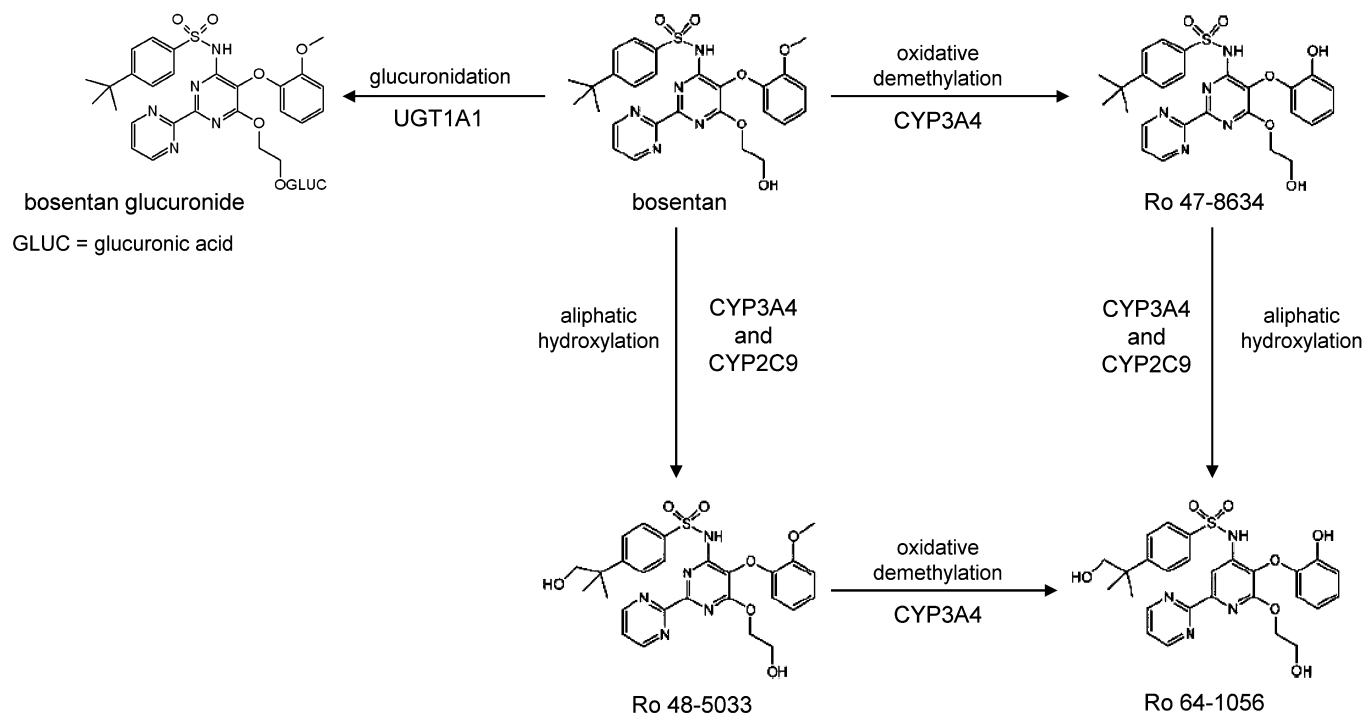
**Figure 7**

Metabolic pathways of bosentan.

ings, Shen *et al*. (2009) mentioned in their abstract minor amounts of conjugates derived from glucuronidation of bosentan itself and of phase I metabolites using human hepatocytes. However, it should be noted that so far, no phase II metabolites of bosentan and its phase I metabolites have been detected in humans.

Currently, we see the primary benefit of the recently generated triple-transfected cell line [expressing OATP1B1, UGT1A1 and MRP2; (Fahrmayr *et al*., 2012)] and the quadruple-transfected cell line described here in the qualitative analysis of the interplay of uptake, metabolism and efflux. For example, phase I or phase II metabolites formed in these cell lines can be studied as MRP2 substrates, whereas this might not be possible using inside-out vesicles of recombinant cells expressing MRP2 due to unavailability of the respective pure compounds. A limitation of these cell lines is that they express with some variability transporters and drug-metabolizing enzymes of particular importance for drug disposition, but certainly not all hepatic proteins affecting hepatic drug handling. Thus, quantitative *in vitro-in vivo* extrapolations should be investigated using other systems such as sandwich-cultured hepatocytes albeit this system has also certain limitations (for review see, e.g. Swift *et al*., 2010).

Taken together, we could demonstrate that it is technically possible to establish a recombinant cell system with the expression of all components necessary for hepatobiliary elimination of drugs. Furthermore, the present study shows that these newly established cell models in addition to primary hepatocytes, animal models and clinical studies represent useful tools to gain more insights into the hepatic disposition of drugs.

## Acknowledgements

## Conflict of interest

Treiber, Pfeifer and Segrestaa are employees of Actelion Pharmaceuticals Ltd (Allschwil, Switzerland).

## References

Artursson P, Karlsson J (1991). Correlation between oral drug absorption in humans and apparent drug permeability coefficients in human intestinal epithelial (Caco-2) cells. Biochem Biophys Res Commun 175: 880–885.

van Aubel RA, Koenderink JB, Peters JG, Van Os CH, Russel FG (1999). Mechanisms and interaction of vinblastine and reduced glutathione transport in membrane vesicles by the rabbit multidrug resistance protein Mrp2 expressed in insect cells. Mol Pharmacol 56: 714–719.

Clozel M, Breu V, Gray GA, Kalina B, Loffler BM, Burri K *et al*. (1994). Pharmacological characterization of bosentan, a new potent orally active nonpeptide endothelin receptor antagonist. J Pharmacol Exp Ther 270: 228–235.

Cole SP, Deeley RG (1998). Multidrug resistance mediated by the ATP-binding cassette transporter protein MRP. Bioessays 20: 931–940.

Cui Y, König J, Buchholz JK, Spring H, Leier I, Keppler D (1999). Drug resistance and ATP-dependent conjugate transport mediated by the apical multidrug resistance protein, MRP2, permanently expressed in human and canine cells. Mol Pharmacol 55: 929–937.

Cui Y, König J, Keppler D (2001). Vectorial transport by double-transfected cells expressing the human uptake transporter SLC21A8 and the apical export pump ABCC2. Mol Pharmacol 60: 934–943.

Dudka J, Jodynis-Liebert J, Korobowicz E, Burdan F, Korobowicz A, Szumilo J et al. (2005). Activity of NADPH-cytochrome P-450 reductase of the human heart, liver and lungs in the presence of (-)-epigallocatechin gallate, quercetin and resveratrol: an in vitro study. Basic Clin Pharmacol Toxicol 97: 74–79.

Evers R, de Haas M, Sparidans R, Beijnen J, Wielinga PR, Lankelma J et al. (2000). Vinblastine and sulfinpyrazone export by the multidrug resistance protein MRP2 is associated with glutathione export. Br J Cancer 83: 375–383.

Fahrmayr C, König J, Auge D, Mieth M, Fromm MF (2012). Identification of drugs and drug metabolites as substrates of multidrug resistance protein 2 (MRP2) using triple-transfected MDCK-OATP1B1-UGT1A1-MRP2 cells. Br J Pharmacol 165: 1836–1847.

Fattinger K, Funk C, Pantze M, Weber C, Reichen J, Stieger B et al. (2001). The endothelin antagonist bosentan inhibits the canalicular bile salt export pump: a potential mechanism for hepatic adverse reactions. Clin Pharmacol Ther 69: 223–231.

Fehrenbach T, Cui Y, Faulstich H, Keppler D (2003). Characterization of the transport of the bicyclic peptide phalloidin by human hepatic transport proteins. Naunyn Schmiedebergs Arch Pharmacol 368: 415–420.

Fouassier L, Kinnman N, Lefevre G, Lasnier E, Rey C, Poupon R et al. (2002). Contribution of mrp2 in alterations of canalicular bile formation by the endothelin antagonist bosentan. J Hepatol 37: 184–191.

Funk C (2008). The role of hepatic transporters in drug elimination. Expert Opin Drug Metab Toxicol 4: 363–379.

van Giersbergen PL, Treiber A, Clozel M, Bodin F, Dingemanse J (2002). In vivo and in vitro studies exploring the pharmacokinetic interaction between bosentan, a dual endothelin receptor antagonist, and glyburide. Clin Pharmacol Ther 71: 253–262.

van Giersbergen PL, Treiber A, Schneiter R, Dietrich H, Dingemanse J (2007). Inhibitory and inductive effects of rifampin on the pharmacokinetics of bosentan in healthy subjects. Clin Pharmacol Ther 81: 414–419.

Glaeser H, Drescher S, van der Kuip H, Behrens C, Geick A, Burk O et al. (2002). Shed human enterocytes as a tool for the study of expression and function of intestinal drug-metabolizing enzymes and transporters. Clin Pharmacol Ther 71: 131–140.

Gomes AM, Winter S, Klein K, Turpeinen M, Schaeffeler E, Schwab M et al. (2009). Pharmacogenomics of human liver cytochrome P450 oxidoreductase: multifactorial analysis and impact on microsomal drug oxidation. Pharmacogenomics 10: 579–599.

Hartman JC, Brouwer K, Mandagere A, Melvin L, Gorczynski R (2010). Evaluation of the endothelin receptor antagonists ambrisentan, darusentan, bosentan, and sitaxsentan as substrates and inhibitors of hepatobiliary transporters in sandwich-cultured human hepatocytes. Can J Physiol Pharmacol 88: 682–691.

Hirouchi M, Kusuhara H, Onuki R, Ogilvie BW, Parkinson A, Sugiyama Y (2009). Construction of triple-transfected cells [organic anion-transporting polypeptide (OATP) 1B1/multidrug resistance-associated protein (MRP) 2/MRP3 and OATP1B1/MRP2/MRP4] for analysis of the sinusoidal function of MRP3 and MRP4. Drug Metab Dispos 37: 2103–2111.

Ho RH, Kim RB (2005). Transporters and drug therapy: implications for drug disposition and disease. Clin Pharmacol Ther 78: 260–277.

Ishiguro N, Maeda K, Saito A, Kishimoto W, Matsushima S, Ebner T et al. (2008). Establishment of a set of double transfectants coexpressing organic anion transporting polypeptide 1B3 and hepatic efflux transporters for the characterization of the hepatobiliary transport of telmisartan acylglucuronide. Drug Metab Dispos 36: 796–805.

Jedlitschky G, Leier I, Buchholz U, Hummel-Eisenbeiss J, Burchell B, Keppler D (1997). ATP-dependent transport of bilirubin glucuronides by the multidrug resistance protein MRP1 and its hepatocyte canalicular isoform MRP2. Biochem J 327 (Pt 1): 305–310.

Jedlitschky G, Hoffmann U, Kroemer HK (2006). Structure and function of the MRP2 (ABCC2) protein and its role in drug disposition. Expert Opin Drug Metab Toxicol 2: 351–366.

Keppler D, Kartenbeck J (1996). The canalicular conjugate export pump encoded by the cmrp/cmoat gene. Prog Liver Dis 14: 55–67.

König J (2011). Uptake transporters of the human OATP family: molecular characteristics, substrates, their role in drug-drug interactions, and functional consequences of polymorphisms. In: Fromm MF, Kim RB (eds). Drug Transporters. Handbook of Experimental Pharmacology 201. Springer-Verlag: Berlin Heidelberg, pp. 1–28.

König J, Cui Y, Nies AT, Keppler D (2000). A novel human organic anion transporting polypeptide localized to the basolateral hepatocyte membrane. Am J Physiol Gastrointest Liver Physiol 278: G156–G164.

König J, Zolk O, Singer K, Hoffmann C, Fromm MF (2011). Double-transfected MDCK cells expressing human OCT1/MATE1 or OCT2/MATE1: determinants of uptake and transcellular translocation of organic cations. Br J Pharmacol 163: 546–555.

Kopplow K, Letschert K, König J, Walter B, Keppler D (2005). Human hepatobiliary transport of organic anions analyzed by quadruple-transfected cells. Mol Pharmacol 68: 1031–1038.

Loe DW, Deeley RG, Cole SP (1998). Characterization of vincristine transport by the M(r) 190 000 multidrug resistance protein (MRP): evidence for cotransport with reduced glutathione. Cancer Res 58: 5130–5136.

Mandery K, Bujok K, Schmidt I, Wex T, Treiber G, Malfertheiner P et al. (2010). Influence of cyclooxygenase inhibitors on the function of the prostaglandin transporter organic anion-transporting polypeptide 2A1 expressed in human gastroduodenal mucosa. J Pharmacol Exp Ther 332: 345–351.

Mano Y, Usui T, Kamimura H (2007). Effects of bosentan, an endothelin receptor antagonist, on bile salt export pump and multidrug resistance-associated protein 2. Biopharm Drug Dispos 28: 13–18.

Nies AT, Herrmann E, Brom M, Keppler D (2008). Vectorial transport of the plant alkaloid berberine by double-transfected cells expressing the human organic cation transporter 1 (OCT1,

SLC22A1) and the efflux pump MDR1 P-glycoprotein (ABCB1). Naunyn Schmiedebergs Arch Pharmacol 376: 449–461.

Patki KC, Von Moltke LL, Greenblatt DJ (2003). In vitro metabolism of midazolam, triazolam, nifedipine, and testosterone by human liver microsomes and recombinant cytochromes p450: role of cyp3a4 and cyp3a5. Drug Metab Dispos 31: 938–944.

Rappa G, Lorico A, Flavell RA, Sartorelli AC (1997). Evidence that the multidrug resistance protein (MRP) functions as a co-transporter of glutathione and natural product toxins. Cancer Res 57: 5232–5237.

Rius M, Hummel-Eisenbeiss J, Hofmann AF, Keppler D (2006). Substrate specificity of human ABCC4 (MRP4)-mediated cotransport of bile acids and reduced glutathione. Am J Physiol Gastrointest Liver Physiol 290: G640–G649.

Seithel A, Eberl S, Singer K, Auge D, Heinkele G, Wolf NB *et al.* (2007). The influence of macrolide antibiotics on the uptake of organic anions and drugs mediated by OATP1B1 and OATP1B3. Drug Metab Dispos 35: 779–786.

Shen G, Yao M, Fura A, Zhu M (2009). *In vitro* metabolite identification and cytochrome P450 reaction phenotyping of bosentan, a dual endothelin receptor antagonist. AAPS J 11 (S2): 001636 (abstract).

Swift B, Pfeifer ND, Brouwer KL (2010). Sandwich-cultured hepatocytes: an in vitro model to evaluate hepatobiliary transporter-based drug interactions and hepatotoxicity. Drug Metab Rev 42: 446–471.

Tamura S, Korzekwa KR, Kimura S, Gelboin HV, Gonzalez FJ (1992). Baculovirus-mediated expression and functional characterization of human NADPH-P450 oxidoreductase. Arch Biochem Biophys 293: 219–223.

Thorin E, Clozel M (2010). The cardiovascular physiology and pharmacology of endothelin-1. Adv Pharmacol 60: 1–26.

Treiber A, Schneiter R, Delahaye S, Clozel M (2004). Inhibition of organic anion transporting polypeptide-mediated hepatic uptake is the major determinant in the pharmacokinetic interaction between bosentan and cyclosporin A in the rat. J Pharmacol Exp Ther 308: 1121–1129.

Treiber A, Schneiter R, Hausler S, Stieger B (2007). Bosentan is a substrate of human OATP1B1 and OATP1B3: inhibition of hepatic uptake as the common mechanism of its interactions with cyclosporin A, rifampicin, and sildenafil. Drug Metab Dispos 35: 1400–1407.

Vermilion JL, Coon MJ (1978). Purified liver microsomal NADPH-cytochrome P-450 reductase. Spectral characterization of oxidation-reduction states. J Biol Chem 253: 2694–2704.

Weber C, Schmitt R, Birnboeck H, Hopfgartner G, van Marle SP, Peeters PA *et al.* (1996). Pharmacokinetics and pharmacodynamics of the endothelin-receptor antagonist bosentan in healthy human subjects. Clin Pharmacol Ther 60: 124–137.

Weber C, Banken L, Birnboeck H, Nave S, Schulz R (1999a). The effect of bosentan on the pharmacokinetics of digoxin in healthy male subjects. Br J Clin Pharmacol 47: 701–706.

Weber C, Gasser R, Hopfgartner G (1999b). Absorption, excretion, and metabolism of the endothelin receptor antagonist bosentan in healthy male subjects. Drug Metab Dispos 27: 810–815.

Weber C, Schmitt R, Birnboeck H, Hopfgartner G, Eggers H, Meyer J *et al.* (1999c). Multiple-dose pharmacokinetics, safety, and tolerability of bosentan, an endothelin receptor antagonist, in healthy male volunteers. J Clin Pharmacol 39: 703–714.

Zolk O, Fromm MF (2011). Transporter-mediated drug uptake and efflux: important determinants of adverse drug reactions. Clin Pharmacol Ther 89: 798–805.